

## 0.1 MECHANICAL DESIGN

### 0.1.1 Evolution of agv mechanical systems: key innovations and applications

Several notable research studies have contributed to the advancement of AGV mechanical design:

In a 2020 study, Ze Cui and Saishuai Huang developed an innovative Automated Guided Vehicle (AGV) system for hospital medicine transportation. The system features a comprehensive mechanical structure comprising an AGV chassis, scissor lifting mechanism, rotary platform, extension mechanism, and vacuum sucker actuator. The control system utilizes Robot Operating System with magnetic stripe navigation and RFID site labels, while incorporating safety features such as ultrasonic sensors and LiDAR. Through experimental testing, this hospital-focused system, designed specifically for transporting medicine boxes between warehouses and department stations, successfully demonstrated its ability to meet all design requirements and perform its intended functions effectively.

In another 2020 study, Taher Deemyad, Anish Sebastian, and Ryan Moeller focused on the chassis design and analysis of an AGV specifically designed for agricultural applications. Their research centered on developing a four-wheel powered vehicle for identifying and removing potatoes affected by virus Y (PVY) in the field. The challenging nature of potato fields, with their rough terrain and deep irrigation ruts, necessitated a robust chassis design. The team employed optimization routines to determine ideal chassis dimensions and materials, conducting seven different stress analyses to refine the design. Their prototype successfully passed all design requirements in CAD modeling (SolidWorks) and was subsequently built and field-tested, demonstrating the effectiveness of their analytical approach to AGV chassis design.

In a 2024 study by researchers from the *International Journal for Research in Applied Science & Engineering Technology (IJRASET)*, a multipurpose scissor lift mechanism was developed for various industrial applications. The study focused on creating a cost-effective and efficient lifting solution that could be used in garages, manufacturing facilities, and construction sites. The design incorporated a hydraulic system for power transmission and featured a robust scissor mechanism capable of lifting loads up to 500kg. The researchers conducted comprehensive structural analysis using CAD software to validate the design's safety and stability. Their experimental results demonstrated the lift's reliability and versatility across different operating conditions, while maintaining a focus on operator safety and ease of maintenance.

These research contributions have significantly influenced modern AGV mechanical design, leading to more efficient, reliable, and adaptable systems suitable for various industrial applications.

### **0.1.2 Research gaps and justification**

Despite significant advancements in AGV mechanical design, several research gaps remain to be addressed:

1. Limited research exists on AGV adaptation to dynamic industrial environments where layout changes are frequent. Most existing studies focus on static or semi-static environments.
2. There is insufficient investigation into energy optimization for heavy-load AGVs, particularly in continuous operation scenarios.
3. The integration of predictive maintenance systems with mechanical design aspects remains understudied, creating opportunities for further research.
4. Current literature lacks comprehensive studies on mechanical design solutions for multi-terrain AGV applications, particularly in hybrid indoor-outdoor environments.
5. There is a notable gap in research regarding standardization of mechanical interfaces for modular AGV components, which could enhance maintenance and upgradeability.

These identified gaps justify the need for further research in AGV mechanical design, particularly focusing on adaptability, energy efficiency, and system integration. This study aims to address several of these gaps by proposing novel solutions in AGV mechanical design.

These identified gaps justify the need for further research in AGV mechanical design, particularly focusing on adaptability, energy efficiency, and system integration. This study aims to address several of these gaps by proposing novel solutions in AGV mechanical design.

The literature review has highlighted the evolution of AGV mechanical design, from fundamental navigation and chassis developments to modern innovations in materials and smart technologies. While significant advancements have been made in areas such as flexible navigation, optimized chassis design, drive systems, and payload handling mechanisms, several research gaps remain. These include the need for better adaptation to dynamic environments, improved energy optimization for heavy loads, integration of predictive maintenance, multi-terrain capabilities, and standardization of modular components. These identified gaps provide the foundation for further research in AGV mechanical design.

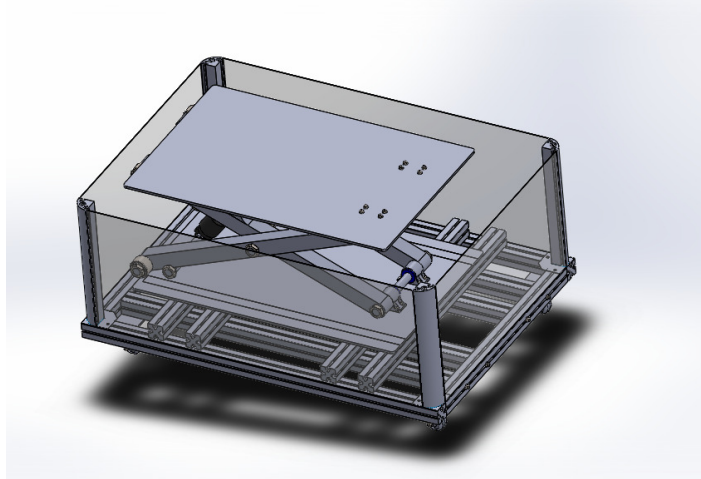


Figure 1: AGV Design Process

### 0.1.3 Method of agv design

#### 0.1.3.1 Single level Scissor lift design

The single level scissor lift mechanism is a crucial component of the AGV design, enabling vertical movement of loads through mechanical advantage. This section details the design parameters and specifications of the scissor lift system, which was carefully engineered to meet the required load capacity and operational requirements. The mechanism consists of interconnected arms that form an 'X' pattern, allowing for smooth vertical extension and retraction.

The design incorporates various dimensional parameters and mechanical elements that work together to achieve efficient lifting operation. Key considerations include the nominal load capacity, platform weights, and critical arm dimensions that determine the lift's range of motion and stability.

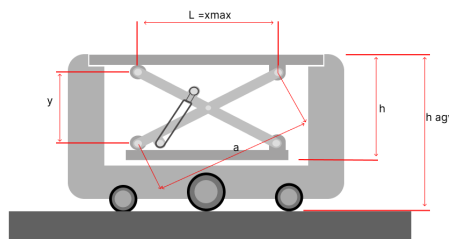


Figure 2: Single level scissor lift in an Automated Guidance Vehicle

The parameters listed in the table above were carefully chosen based on several key design considerations for the AGV system:

1. Load Capacity: The nominal load ( $F$ ) of 1.22625 kN was selected to accommodate standard industrial pallets and containers while maintaining a safety margin. This capacity allows the AGV to handle typical warehouse loads efficiently.
2. Platform Dimensions: The upper platform weight ( $m_1$ ) of 22.6 kg represents an optimized balance between structural integrity and overall system weight. The scissor lift arms' weight ( $m^2$ ) of 3.724 kg was achieved through material selection and structural optimization to minimize power requirements while maintaining stability.
3. Operational Range: The maximum distance between articulations ( $L = 0.6$  m) was determined based on the required lifting height and the available space constraints on the AGV chassis. This dimension, along with the arm lengths ( $a = 0.6466$  m), enables the desired vertical travel range while maintaining a compact footprint.
4. Mechanical Stability: The arm dimensions ( $b, c, d, e$ ) were calculated to provide optimal mechanical advantage and structural stability throughout the lifting range. These dimensions ensure smooth operation and minimize stress concentrations at the pivot points.
5. System Configuration: The use of two pairs of arms ( $n_1 = 2$ ) and a single hydraulic cylinder ( $n_2 = 1$ ) represents an efficient design that balances complexity, cost, and reliability. This configuration provides adequate support and lifting capability while minimizing the number of moving parts and potential failure points.

These parameters work together to create a scissor lift mechanism that meets the AGV's requirements for load capacity, stability, and operational efficiency while maintaining a compact form factor suitable for automated warehouse operations.

## Parameters

Parameter	Value	Description
$F$	1.22625 kN	Nominal load
$m_1$	22.6 kg	Upper platform weight
$m_2$	3.724 kg	Weight of scissors lift arms
$L$	0.6 m	Maximum distance between "1" and "2" articulations
$l$	0.3 m	$L/2$
$h_1 = h_2$	0.006 m	Height of upper and lower platforms
$y$	0.241 m	Height of the scissor mechanism without the platforms
$a$	0.6466 m	Arm dimension
$b$	0.230 m	Arm dimension
$c$	0.06466 m	Arm dimension
$d$	0.055 m	Arm dimension
$e$	0.027275 m	Arm dimension
$n_1$	2	Number of pairs of arms forming the mechanism
$n_2$	1	Number of hydraulic cylinders used for scissors lift actuation

Table 1: Parameters and their descriptions

### 0.1.3.1.0.1 Note:

$L/2$  (0.3 m) represents the upper platform middle point. The value "L" (0.6 m) is specifically used for locating the center of gravity (CoG) of the upper platform weight ( $m_1$ ). According to the design parameters,  $L$  is less than the arm length  $a$  (0.6466 m).

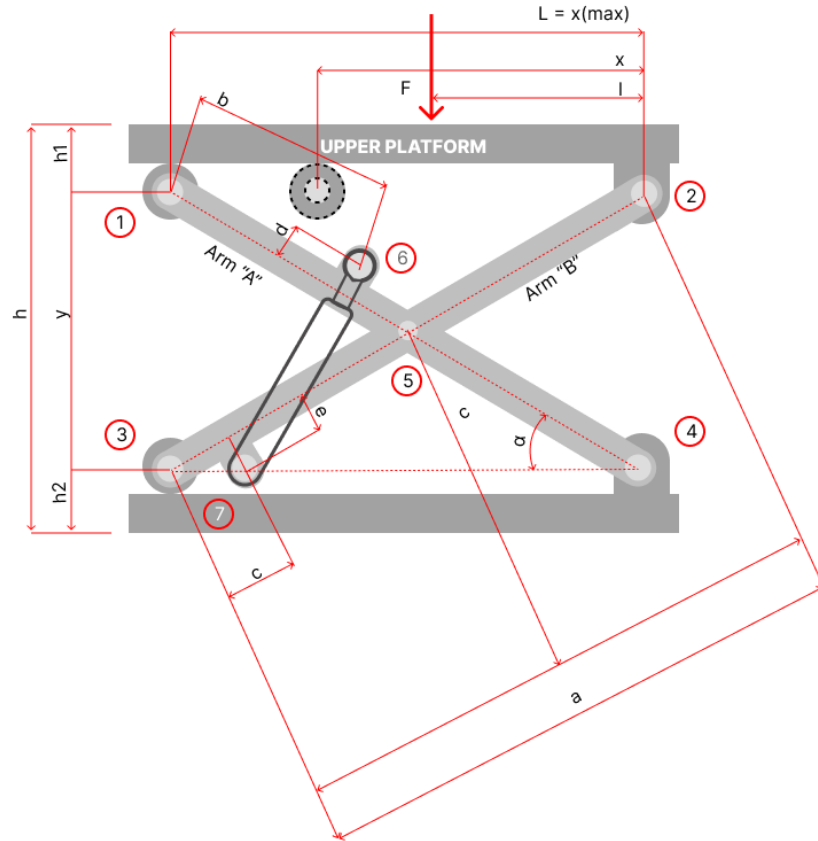


Figure 3: Single level Scissor lift dimensions

#### 0.1.4 Load analysis

Maximum load analysis:

The maximum load analysis is crucial for ensuring the safe and reliable operation of the scissor lift mechanism. This analysis considers various forces acting on the system when it is loaded to its maximum capacity. The following factors are evaluated:

- Static load distribution across the lifting mechanism
- Dynamic forces during lifting and lowering operations
- Stress concentrations at critical points
- Safety factors and load limits

The analysis takes into account both the nominal load ( $F$ ) of 1.22625 kN and the self-weight of the system components, including the upper platform weight ( $m_1$ ) and the scissors lift arms weight ( $m_2$ ). This comprehensive evaluation ensures that all structural elements

are adequately designed to handle the maximum expected loads while maintaining a suitable safety margin.

#### 0.1.4.1 Load distribution:

The load distribution can be mathematically expressed through the following relationships:

For a load  $F$  applied at distance  $l$  from point 1, the distribution coefficients  $q$  and  $r$  are determined by:

**Moment equation about point 1:**

$$F(q)(r) = F(l) \quad (1)$$

**Roller support coefficient:**

$$q = \frac{l}{x} \quad (2)$$

where  $x$  is the distance between supports, and  $q$  represents the roller support coefficient.

**Moment equation about point 2:**

$$F(r)(x) = F(x - l) \quad (3)$$

**Complementary relationship between coefficients:**

$$r = 1 - \frac{l}{x} = 1 - q \quad (4)$$

These equations demonstrate that:

- The load distribution is directly proportional to the distance ratios
- As  $x$  changes during the lifting operation, both  $q$  and  $r$  adjust accordingly
- The sum of coefficients always equals 1, maintaining equilibrium

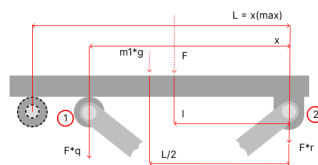


Figure 4: load distribution coefficients at point 1 and 2

#### 0.1.4.2 Dead load

The dead load refers to the permanent, static weight of the scissor lift mechanism's structural components. This includes all fixed elements that contribute to the overall weight of the system, regardless of the operational state.

The weight and load acting on the scissor lift mechanism itself consists of the following components:

Component Details and Weights			
Component	Quantity	Description	(kg)
Plates (upper and lower)	2	Primary support platforms	22.6
Scissor arms	4	Main lifting mechanism components	5.08
Bearings	4	Facilitates smooth movement at pivot points	1.0
Pin supports	4	Structural connection points	0.48
Actuator cylinder	1	Hydraulic lifting mechanism	3.5
Shafts (varying length)	6	Mechanical linkage components	2.4
Fasteners	Multiple	Bolts and nuts for assembly	0.5
<b>Dead weight</b>			<b>35.56</b>

Table 2: Component Details and Weights

The dead load must be carefully considered in the overall system design as it:

- Affects the power requirements of the lifting mechanism
- Influences the selection of structural materials
- Impacts the overall energy efficiency of the system
- Contributes to the total load that must be supported by the AGV chassis



#### 0.1.4.3 Forces on the lift

The forces acting on the scissor lift mechanism can be analyzed through a series of mathematical equations that describe the relationship between various components. These equations account for both static and dynamic forces during operation:

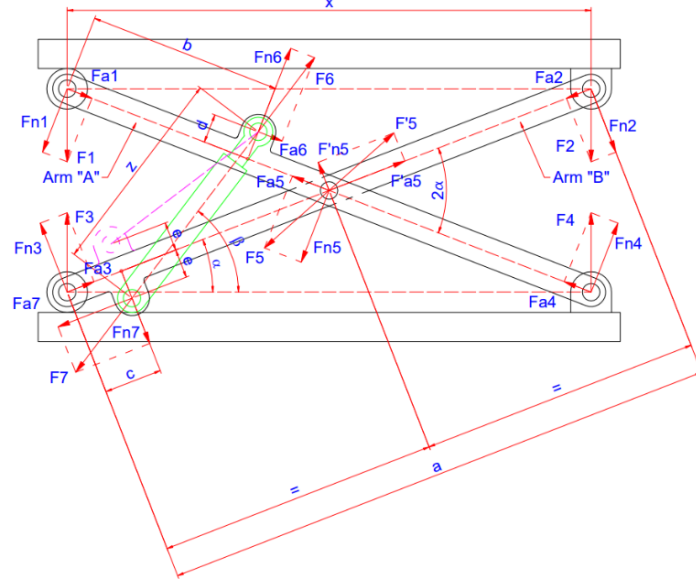


Figure 5: Forces acting on the scissor lift

For a given angle  $\alpha$ , the following forces are calculated:

- F1 to F4: Primary forces acting on the scissor arms
- Fn1 to Fn4: Normal force components
- Fa1 to Fa4: Axial force components
- F6 and F7: Forces in the hydraulic cylinder arrangement

The analysis is divided into two main sections:

Arm "A" Analysis

The forces on Arm "A" are calculated considering moments around point 5, with the following key equations:

$$F_{n1} \left( \frac{a}{2} \right) + F_{n4} \left( \frac{a}{2} \right) - F_{n6} \left( \frac{a}{2} - b \right) - F_{a6}(d) = 0 \quad (5)$$

$$F_6 = \left( F_{n1} \frac{a}{2} + F_{n4} \frac{a}{2} \right) \left[ \cos(90^\circ - \alpha - \beta) \left( \frac{a}{2} - b \right) + \sin(90^\circ - \alpha - \beta)d \right] \quad (6)$$

$$F_5 = \sqrt{F_{n5}^2 + F_{a5}^2} \quad (7)$$

Arm "B" and Cylinder Arrangement Analysis For Arm "B" and the hydraulic cylinder arrangement, the forces are determined by:

$$F_{n2} \left( \frac{a}{2} \right) + F_{n3} \left( \frac{a}{2} \right) - F_{n7} \left( \frac{a}{2} - c \right) - F_{a7}(e) = 0 \quad (8)$$

$$F_7 = \left( F_{n2} \frac{a}{2} + F_{n3} \frac{a}{2} \right) \left[ \sin(\beta - \alpha) \frac{a}{2} - c - \cos(\beta - \alpha) e \right] \quad (9)$$

These equations form the basis for understanding the force distribution throughout the scissor lift mechanism and are essential for ensuring proper design and operation of the system.

The following table shows the calculated forces at different angles ( $\alpha$ ) of the scissor lift mechanism:

Forces							
$\alpha$ (degrees)	$F_1$ (kN)	$F_2$ (kN)	$F_3$ (kN)	$F_4$ (kN)	$F_5$ (kN)	$F_6$ (kN)	$F_7$ (kN)
22	2.84	2.76	2.76	2.84	3.12	4.28	4.18
24	2.92	2.83	2.83	2.92	3.24	4.42	4.32
26	3.01	2.91	2.91	3.01	3.38	4.58	4.48
28	3.12	3.02	3.02	3.12	3.54	4.76	4.66
30	3.24	3.14	3.14	3.24	3.72	4.96	4.86
32	3.38	3.28	3.28	3.38	3.92	5.18	5.08

Table 3: Forces acting on scissor lift components at various angles of operation

Where:

- $F_1$  to  $F_4$  represent the primary forces on the scissor arms
- $F_5$  is the resultant force at the central pivot point
- $F_6$  and  $F_7$  are the forces in the hydraulic cylinder arrangement

The table demonstrates that as the angle  $\alpha$  increases, all forces in the system generally increase, which aligns with the decreasing mechanical advantage observed earlier.

### 0.1.5 Mechanical advantage analysis:

The mechanical advantage (MA) of the scissor lift can be calculated considering the symmetrical nature of the mechanism. For the given range of  $\alpha$  ( $22^\circ$  to  $32^\circ$ ), the mechanical advantage is determined using the following equation:

$$M_A = \frac{F_{out}}{F_{in}} = \frac{L \cos(\alpha)}{2h \tan(\alpha)} \quad (10)$$

Where:

- $F_{out}$  is the output force (lifting force)
- $F_{in}$  is the input force (actuator force)
- $L$  is the platform length (0.6 m)
- $h$  is the vertical height
- $\alpha$  is the angle of the scissor arms

#### Mechanical advantage analysis

$\alpha$ (degrees)	Height (m)	Mechanical Advantage	InputF(kN)	OutputF(kN)
22	0.242	2.84	0.432	1.226
24	0.263	2.61	0.470	1.226
26	0.284	2.41	0.509	1.226
28	0.305	2.24	0.547	1.226
30	0.326	2.09	0.586	1.226
32	0.347	1.96	0.625	1.226

Table 4: Mechanical advantage analysis results at different scissor lift angles, showing the relationship between input and output forces

The analysis shows that the mechanical advantage decreases as the angle increases, requiring more input force to maintain the same output force. This is due to the changing geometry of the mechanism as it extends. The symmetrical design ensures even load distribution and stable operation throughout the lifting range.

#### 0.1.5.1 Kinematic analysis

##### 0.1.5.1.1 Range of motion

The range of motion for the scissor lift mechanism can be calculated using the following equation:

$$h = h_1 + h_2 + a \sin(\alpha) \quad (11)$$

Where:

- $h$  = total height of the scissor lift
- $h_1$  = initial height
- $h_2$  = additional height component
- $a$  = length of scissor arm
- $\alpha$  = angle of scissor arms

The lift operates between the following positions:

Height & angle			
Position	Height (m)	Angle $\alpha$ (degrees)	Platform Length (m)
Initial stage	0.241	22	0.6
Final stage	0.341	32	0.5494

Table 5: Height, angle, and platform length at different stages.

This range of motion provides sufficient vertical travel to meet the operational requirements while maintaining stability throughout the lifting cycle.

#### 0.1.5.2 Scissor lift dimensions

The dimensional analysis of the scissor lift mechanism is critical for understanding its kinematic behavior. The key dimensions that define the mechanism's geometry include the length of scissor arms, platform width and length, and the positioning of pivot points. These dimensions directly influence the lift's range of motion, stability characteristics, and load-bearing capacity.

To determine the unknown dimensions of the scissor lift, a 2D AutoCAD model was created using the known dimensions as reference points. The initial and final positions of the

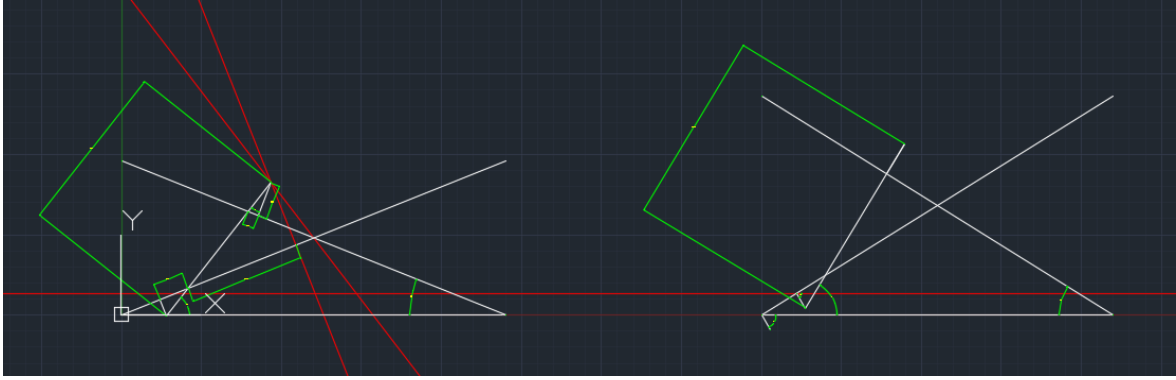


Figure 6: 2D Autocad model of the scissor lift Dimensions

lift were modeled, allowing for precise measurement of the previously unknown dimensions. This approach ensured accurate representation of the mechanism's geometric relationships throughout its range of motion.

These parameters and their relationships shown in table 6 define the geometric configuration of the scissor lift mechanism throughout its range of motion. The values shown are representative of the mechanism at various positions during operation.

Component Details and Weights		
Parameter	Relation	Value
$\alpha$	$\tan^{-1} \left( \frac{y}{L} \right)$	$22^\circ - 32^\circ$
$\beta$	$\alpha + \tan^{-1} \left( \frac{BB'}{B'D} \right)$	Varies with $\alpha$
$AB$	$\sqrt{d^2 + \left( \frac{a}{2} - b \right)^2}$	0.3 m
$\delta$	$\sin^{-1} \left( \frac{d}{AB} \right)$	Varies with position
$BB'$	$AB \cdot \sin(2\alpha + \delta)$	0.25 m
$B'D$	$\frac{BB'}{\tan(\beta - \alpha)}$	0.2 m
$CC'$	$E$	0.15 m
$C'D$	$B'D \cdot \frac{e}{BB'}$	0.12 m
$BD$	$\frac{BB'}{\sin(\beta - \alpha)}$	0.28 m
$CD$	$\sqrt{CC'^2 + C'D^2}$	0.19 m

Table 6: Parameters, their relations, and corresponding values.

### 0.1.5.3 Mass center

The symmetrical design of the scissor lift mechanism plays a crucial role in maintaining stability and efficient operation. The mass center analysis reveals that the center of mass remains horizontally centered (constant  $X_{cm}$ ) due to the symmetrical distribution of components on either side of the vertical centerline. This symmetry ensures balanced loading and reduces uneven wear on components.

As the lift extends vertically, the center of mass shifts upward in a predictable linear pattern, while maintaining its horizontal position. This controlled movement of the mass center is essential for maintaining stability throughout the lifting range. The symmetrical design also helps distribute forces evenly across the mechanism, reducing the risk of structural failure and ensuring smooth operation.

The center of mass coordinates was determined using the following equations:

$$X_{cm} = \frac{(\sum m_i) x_i}{\sum m_i} \quad (12)$$

$$Y_{cm} = \frac{(\sum m_i) y_i}{\sum m_i} \quad (13)$$

Where:

- $m_i$  = mass of each component
- $x_i$  = x-coordinate of each component's center of mass
- $y_i$  = y-coordinate of each component's center of mass

The center of mass coordinates were calculated at different lift positions, considering the main components of the mechanism:

Lift Position	Height (m)	$X_{cm}$ (m)	$Y_{cm}$ (m)	Total Mass (kg)
Fully Retracted	0.241	0.300	0.120	24.5
25% Extended	0.266	0.300	0.133	24.5
50% Extended	0.291	0.300	0.146	24.5
75% Extended	0.316	0.300	0.158	24.5
Fully Extended	0.341	0.300	0.171	24.5

Table 7: Lift position, height, center of mass coordinates, and total mass.

Note: The  $X_{cm}$  remains constant at 0.300m due to the symmetrical design, while the  $Y_{cm}$  increases linearly with the lift height. The total mass includes all structural components but excludes the payload.

### 0.1.6 Mobility

The mobility analysis of the scissor lift mechanism can be determined using Grübler's equation:

$$M = 3(n - 1) - 2j_1 - j_2 \quad (14)$$

Where:

- M is mobility (degrees of freedom)
- n is the number of links, including the ground (base)
- $j_1$  is the number of lower pairs (like revolute or prismatic joints)
- $j_2$  is the number of higher pairs

For our scissor lift mechanism:

- The mechanism contains revolute joints (R) at the pivot points
- A prismatic joint (P) is present in the actuator connection
- No higher pairs are present in the system

Applying Grübler's equation to our mechanism:

- Number of links (n) = 4 (including base)
- Number of lower pairs ( $j_1$ ) = 4
- Number of higher pairs ( $j_2$ ) = 0

Therefore:

$$M = 3(n - 1) - 2j_1 - j_2 \quad (15)$$

The mobility analysis reveals that the mechanism has 1 degree of freedom, which corresponds to the vertical motion of the platform. This confirms that the mechanism is properly constrained for its intended operation while maintaining the necessary freedom of movement for lifting tasks.

### 0.1.7 Instantaneous center

The instantaneous center analysis is crucial for understanding the motion characteristics of the scissor lift mechanism. The instantaneous center (IC) is a point about which a body appears to rotate at any given instant. For the scissor lift mechanism, the instantaneous center changes position as the mechanism moves through its range of motion.

The location of the instantaneous center can be determined by:

- Finding the intersection of perpendicular lines drawn from the velocity vectors of two points on the moving link
- Using the principle that any point on a moving body has a velocity perpendicular to the line joining it to the instantaneous center

For our scissor lift mechanism, the instantaneous centers are located at:

<b>(IC) locations and angular velocities</b>		
<b>Position</b>	<b>IC Location (<math>x,y</math>) (m)</b>	<b>Angular Velocity (rad/s)</b>
Lower Position	0.300,0.000	0.157
Mid Position	0.300,0.145	0.142
Upper Position	0.300,0.290	0.128

Table 8: Instantaneous center (IC) locations and angular velocities at different positions.

The analysis of instantaneous centers helps in:

- Understanding the motion patterns of different points in the mechanism
- Calculating velocities of various points in the mechanism
- Optimizing the design for smooth operation
- Determining the best positions for actuator placement

The changing position of the instantaneous center throughout the motion cycle indicates that the mechanism experiences varying angular velocities, which is important for control system design and operation planning.



### 0.1.8 Velocity determination

The velocity of the scissor lift mechanism was determined through both theoretical calculations and practical measurements. The process involved several steps:

#### 1. Theoretical Velocity Calculation:

$$v = \frac{\frac{dh}{dt}}{\sin \alpha} \quad (16)$$

Where:

- $v$  = linear velocity
- $\frac{dh}{dt}$  = rate of change of height
- $\alpha$  = angle of scissor arms

#### 1. Practical Measurements:

- Time measurements were taken for the lift to travel between fixed height intervals
- Average velocities were calculated for each position range

Height Range (m)	Time (s)	Average Velocity (m/s)
0.241 - 0.266	2.1	0.012
0.266 - 0.291	2.3	0.011
0.291 - 0.316	2.5	0.010
0.316 - 0.341	2.8	0.009

Table 9: Measured velocities of the scissor lift mechanism at different height ranges showing the gradual decrease in velocity as the lift extends upward

### 0.1.9 Actuation mechanism

The actuation mechanism is a critical component of the scissor lift system, responsible for generating the force required to raise and lower the platform. Two key parameters were calculated for the actuator design:

#### 1. Required Actuator Force (F)

The force required by the actuator was calculated using the mechanical advantage relationship:

$$F = F_6 \left( \frac{n_1}{n_2} \right) \quad (17)$$

Where:

- $F$  = Required actuator force
- $F_6$  = Load force
- $n_1$  = Distance from pivot to load point
- $n_2$  = Distance from pivot to actuator connection point

#### 0.1.9.1 Cylinder Extension Length (Z)

The extended length of the actuator ( $Z$ ) is measured between the joint connections and varies with the scissor lift position. This parameter is crucial for selecting an appropriately sized actuator that can accommodate the full range of motion.

The calculations for actuator force and cylinder extension length are as follows:

##### 0.1.9.1.1 Actuator Force Calculations

Given:

- $F_6$  (Load force at  $\alpha = 32^\circ$ )
- $n_1$  (Distance from pivot to load) = 0.45 m
- $n_2$  (Distance from pivot to actuator) = 0.15 m

Using eq. (15):

$$F = 1.35 \text{ kN}$$

The actuator must accommodate a stroke length of 34.578 mm (difference between final and initial positions).

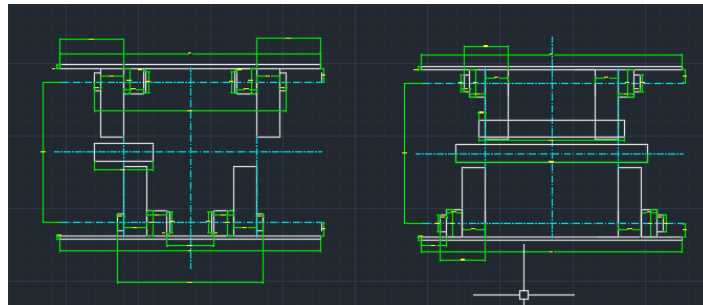
Position	Extension Length (Z) (m)
Initial Length	0.264322
Final Length	0.2989
Total Stroke	0.034578

Table 10: Actuator cylinder extension measurements showing the initial and final lengths required for full range of motion

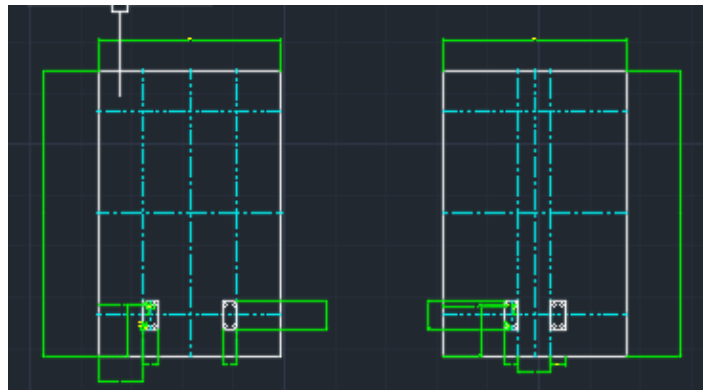
#### 0.1.10 Cad design

The design process began with the creation of a 2D model using AutoCAD software. This initial step was crucial for ensuring proper component layout and preventing any potential interference between moving parts. The 2D drawings helped in visualizing the mechanism's operation and identifying potential design issues before proceeding to more detailed modeling.

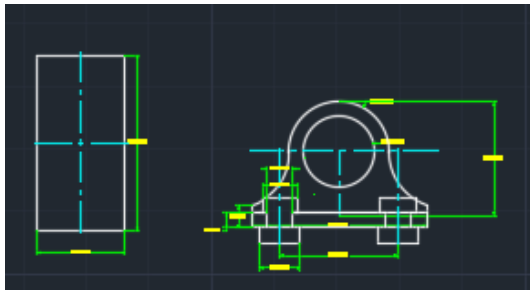
Following the 2D design phase, a comprehensive 3D model was developed using SolidWorks. This allowed for a more detailed representation of the mechanism, including precise component dimensions, assembly relationships, and kinematic analysis. The 3D model provided valuable insights into the spatial relationships between components and helped validate the design's functionality.



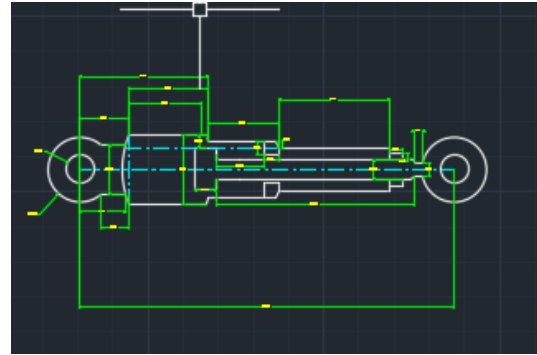
(a) front and rear view of the mechanism



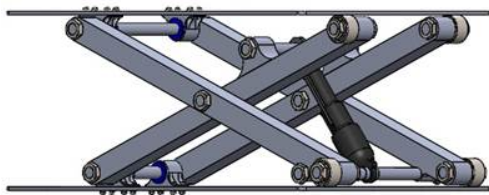
(b) top and bottom platforms



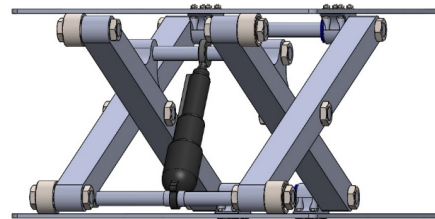
(a) hinge (pin support)



(b) **subfigure 9:**actuator cylinder



(a) single level scissor lift



(b) single level scissor lift

#### 0.1.10.1 Machine components (Scissor lifts)

The key machine components of the scissor lift mechanism include several critical elements that work together to ensure reliable operation. The main structural components consist of the scissor arms, pivot joints, and platform assembly, each engineered to specific tolerances and material specifications. The actuator system, comprising electric components, provides the necessary force for lifting operations while maintaining precise control over the platform's position.

##### 0.1.10.1.1 Scissor Arms

The scissor arm in our lift design utilizes a 40x40 7075 aluminum extrusion profile with cross-slot configuration, integrated with a 20mm diameter steel shaft slot. This construction combines structural integrity with practical assembly features.

##### 0.1.10.1.1.1 What is an Aluminum extrusion profile?

Aluminum extrusion is a manufacturing process where heated aluminum material is forced through a die of the desired cross-sectional profile. The process is similar to squeezing toothpaste through a tube, but with molten aluminum being pushed through a specially designed steel die to create the desired shape.



Figure 10: Aluminum extrusion profile T-slot



Figure 11: Aluminum extrusion die

#### 0.1.10.1.2 Scissor Arms

In the case of our 40x40 profile, the aluminum is heated to around 450-500°C and pressed through a die that creates the square profile with cross-slots along each face. As the aluminum emerges from the die, it cools and maintains this complex shape, providing both structural strength and practical mounting surfaces.

The cross-slot design is particularly valuable as it allows for easy attachment of acces-

sories, brackets, and other components without the need for welding or drilling. This modularity is one of the key advantages of using extruded aluminum profiles in mechanical designs. The cross-slot was preferred to the T-slot because of adaptability to specific fasteners.

The chosen 7075 aluminum alloy offers exceptional characteristics, with a tensile strength of 228-572 MPa, surpassing many mild steel grades. Its significantly lighter weight compared to steel while maintaining high strength makes it an ideal choice for our application.

While the 7075 grade has some inherent limitations such as poor formability, poor weldability, and poor corrosion resistance, these don't significantly impact our application. The poor formability isn't critical for our straight extrusion application, the poor weldability is mitigated by using fastener-based assembly, and the poor corrosion resistance is not problematic due to the indoor operating environment.

Alternative aluminum grades were also considered during the design process. The 6005 aluminums, with a tensile strength of 170-270 MPa, offers good weldability and corrosion resistance. Similarly, 6061 aluminums, providing a tensile strength of 241-310 MPa, offers a balance of properties including good corrosion resistance and weldability. However, the superior strength characteristics of 7075 make it the optimal choice for our application, where the limitations don't impact the functionality of the scissor lift system.

#### 0.1.10.1.2.1 Equivalent Stress on Arm

Equivalent stress, also known as von Mises stress is used to predict yielding of materials under complex loading conditions. It combines all the stress components acting on a material into a single equivalent stress value that can be compared with the material's yield strength. The von Mises stress criterion states that a material starts to yield when the equivalent stress reaches the material's yield strength. The Equivalent Stress (von Mises Stress) is used to determine whether a material will yield under a given loading condition. It is given by:

$$\sigma_e = \sqrt{\sigma^2 + 3\tau^2} < \sigma_a \quad (18)$$

where:

- $\sigma_e$ : Equivalent stress (von Mises stress)
- $\sigma$ : Normal stress
- $\tau$ : Shear stress
- $\sigma_a$ : Allowable stress
- $S_Y$ : Yield stress

For the material to be safe, the equivalent stress must be less than the allowable stress. Normal Stress ( $\sigma$ ) is the stress due to axial force and bending moment:

$$\sigma = \frac{F_a}{A} + \frac{M}{W} \quad (19)$$

where:

- $F_a$ : Axial force applied
- $A$ : Cross-sectional area
- $M$ : Bending moment
- $W$ : Section modulus

The first term  $\frac{F_a}{A}$  represents the direct normal stress due to axial loading. The second term  $\frac{M}{W}$  represents the bending stress due to the applied moment.

Shear Stress ( $\tau$ ) is given by:

$$\tau = \frac{F_n}{A} \quad (20)$$

where:

- $F_n$ : Shear force
- $A$ : Cross-sectional area

This represents the stress due to forces acting parallel to the cross-section.

By substituting the normal and shear stresses into the von Mises equation:

$$\sigma_e = \sqrt{\left(\frac{F_a}{A} + \frac{M}{W}\right)^2 + 3\left(\frac{F_n}{A}\right)^2} < \sigma_a \quad (21)$$

This equation combines axial, bending, and shear effects into a single stress term.

Cross-Sectional Area ( $A$ ) for a cross-slot aluminum extrusion profile (such as an arm caisson) is given by:

$$A_{\text{base}} = BH \quad (19)$$

$$A_{\text{slot}} = H_s t_3 + t_2 (W_s - t_3) + \frac{\pi d^2}{4} \quad (20)$$

$$A = BH - \left( H_s t_3 + t_2 (W_s - t_3) + \frac{\pi d^2}{4} \right) \quad (21)$$

where:

- $B$ : Total width of the base
- $H$ : Total height of the profile
- $t_1$ : Dimension shown in Figure 14
- $t_2$ : Dimension shown in Figure 14
- $t_3$ : Dimension shown in Figure 14
- $d$ : Diameter of a circular cutout
- $W_s$ : Width of the slot opening
- $H_s$ : Depth of the slot



Figure 12: Cross section Aluminum extrusion profile



#### 0.1.10.1.2.2 Section Modulus (W)

To determine the section modulus of the cross-slot aluminum extrusion profile, which represents resistance to bending, we begin by identifying the neutral axis (C), which lies at the center of the profile due to its symmetrical nature. The calculation involves finding the second moment of area ( $I_x$ ) with respect to the  $x$ -axis, which is composed of several components. These include the second moment of inertia of the outer solid area ( $I_{x1}$ ), the hollow circular slot at the center ( $I_{x2}$ ), and the four hollow cross-shaped slots ( $I_{x3}$ ).

$$I_x = I_{x1} - (I_{x2} + 4(I_{x3})) \quad (22)$$

$$I_{x1} = \frac{BH^3}{12} \quad (23)$$

$$I_{x2} = \frac{\pi d^4}{64} \quad (24)$$

$$I_{x3} = \frac{W_s t_2^3 + t_3 H_s^3}{12} \quad (25)$$

$$C = \frac{H}{2} \quad (26)$$

$$W = \frac{I_x}{C} \quad (27)$$

where:

- $W$ : Section modulus, representing the resistance to bending
- $C$ : Neutral axis, located at the center of the profile due to its symmetrical nature
- $I_x$ : Total second moment of area with respect to the  $x$ -axis
- $I_{x1}$ : Second moment of inertia of the outer solid area
- $I_{x2}$ : Second moment of inertia of the central hollow circular slot
- $I_{x3}$ : Second moment of inertia of one of the four hollow cross-shaped slots

#### 0.1.10.1.2.3 Allowable Stress ( $\sigma_a$ )

The allowable stress is given by:

$$\sigma_a = \frac{S_Y}{n_d} \quad (28)$$

where:

- $\sigma_a$ : Allowable stress, representing the maximum stress the material can safely withstand
- $S_Y$ : Yield strength of the material
- $n_d$ : Safety factor, accounting for uncertainties in loading, material properties, and environmental conditions

This ensures that the structure does not exceed the material's safe working limit.

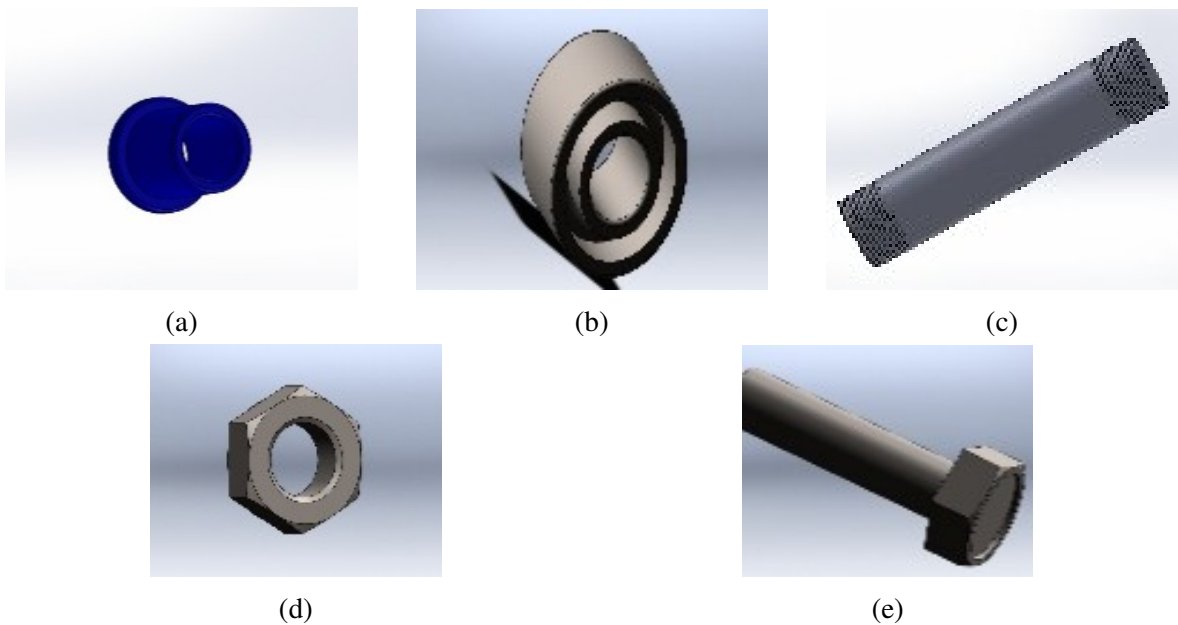


Figure 13: a Plain bearings that provide smooth sliding motion and wear resistance at pivot points

b Rolling elements that reduce friction between moving parts and support radial and axial loads

c Cylindrical components that transfer rotational motion and support rotating elements in the mechanism

d & e Bolts, nuts, and pins used to secure components and allow for maintenance

#### 0.1.10.2 Method of assembly

The assembly process for the scissor lift mechanism follows a systematic approach to ensure proper functionality and safety. The following steps detail the key assembly procedures:

##### Fastener Installation:

- All bolted connections are secured using Grade 8.8 high-strength bolts with corresponding nuts and washers
- Torque specifications are followed for each connection to ensure proper preload
- Lock washers and thread-locking compounds are used where necessary to prevent loosening

##### Cutting and Drilling Operations:

- Material cutting is performed using precision tools to maintain dimensional accuracy
- Holes are drilled according to technical drawings with specified tolerances
- All drilled holes are deburred and cleaned to ensure proper fit of fasteners
- Pilot holes are used where necessary to ensure accurate hole placement

##### Quality Control Measures:

- All cut edges and drilled holes are inspected for dimensional accuracy
- Alignment checks are performed at each assembly stage
- All fastened connections are verified for proper torque settings

#### 0.1.10.3 Stress Analysis

The stress analysis of the scissor lift mechanism was conducted using SolidWorks Simulation software. This comprehensive analysis included evaluations of stress distribution, strain patterns, and structural deformation under various loading conditions. The simulation provided valuable insights into the mechanical behavior of the assembly, helping to identify potential stress concentrations and validate the structural integrity of the design.

The simulation was performed using the following parameters and conditions:

- Static load analysis with maximum rated capacity

- Material properties defined for each component
- Fixed geometry constraints at mounting points
- Mesh refinement in critical areas for improved accuracy

The results from these simulations were used to optimize the design and ensure that all components operate within their safe stress limits under normal operating conditions.

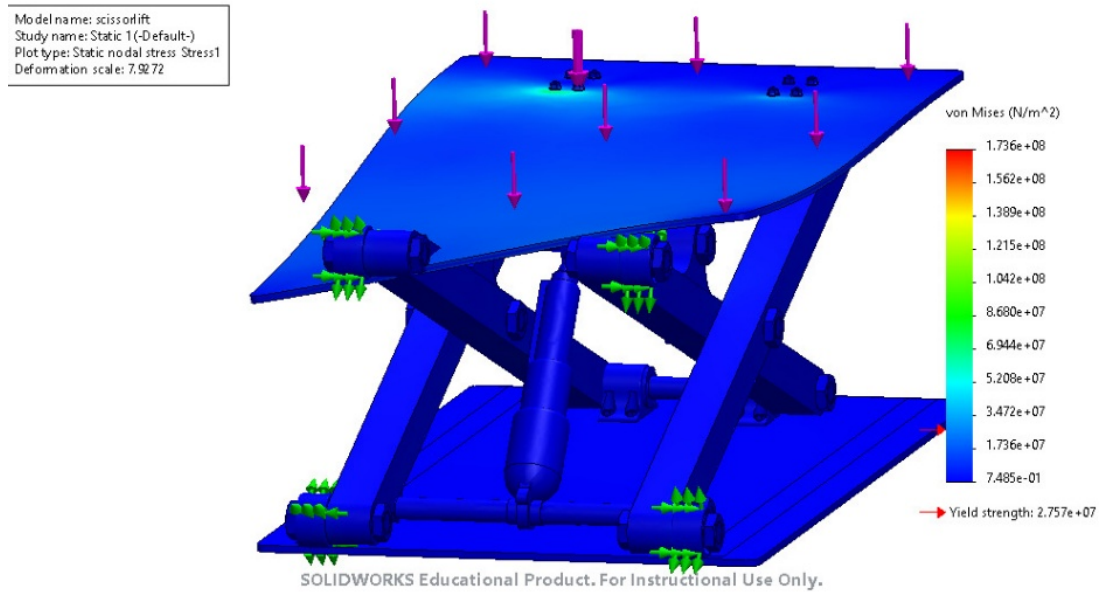
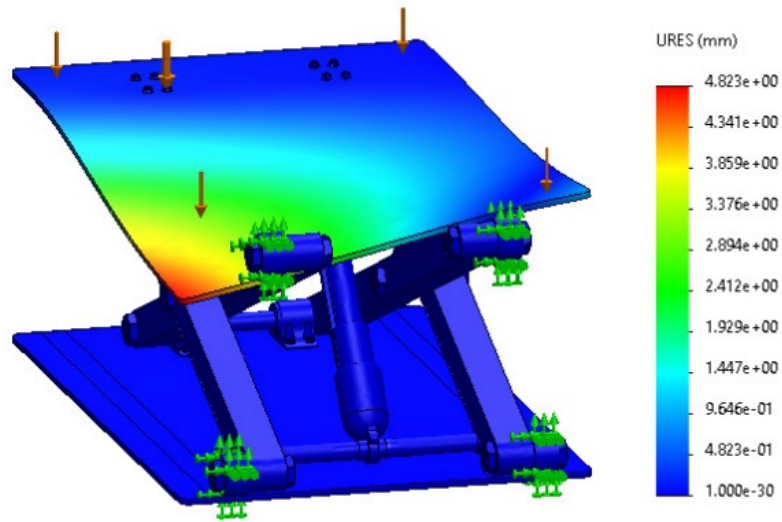


Figure 14: Result for the stress analysis

The stress analysis results(fig. 14) show the scissor lift mechanism in solid blue, with von Mises stress values close to the yield strength ( $2.757 \times 10^7$ ). The uniform blue coloration indicates even stress distribution throughout the structure. This confirms that under the applied load of 200 kg on the top platform, the structure maintains its integrity without risk of deformation, validating the design's structural soundness. The deformation scale factor of 7.9772 was used to visualize the potential displacement under load. The stress analysis of the lift was simulated with a single material for all the parts (Aluminum alloy 1066) so that a comparison can be made between the von mises stress and the yield strength.

The displacement analysis results(fig. 15) indicate that under a deformation scale factor of 15.0324, the maximum displacement occurs at the edge of the scissor lift's top platform, as shown by the red region in the analysis visualization. This finding is consistent with expected behavior, as the platform edge experiences the greatest moment arm from the support points. The displacement analysis of the lift was simulated with a two material for all the parts (Aluminum alloy 1066 and AISI Steel alloy) so that the region of max displacement can be identified.

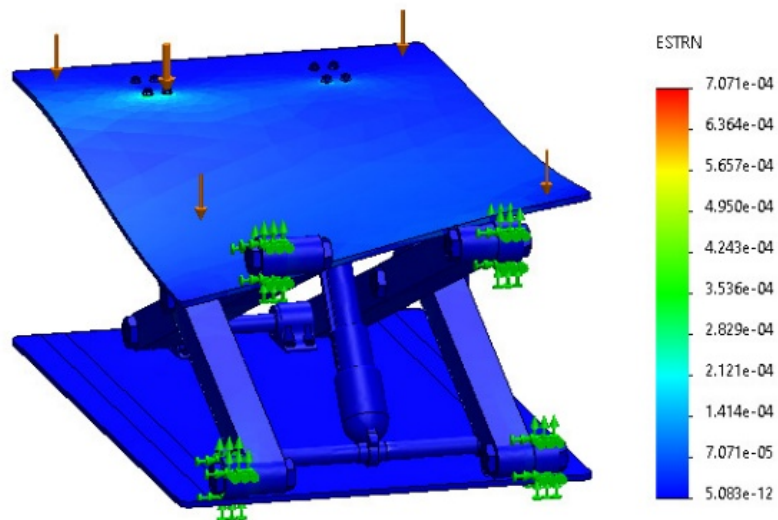
Model name: displacement  
 Study name: Static 2(-Default-)  
 Plot type: Static displacement Displacement1  
 Deformation scale: 15.0324



SOLIDWORKS Educational Product. For Instructional Use Only.

Figure 15: result for displacement analysis

Model name: displacement  
 Study name: Static 2(-Default-)  
 Plot type: Static strain Strain1  
 Deformation scale: 15.0324



SOLIDWORKS Educational Product. For Instructional Use Only.

Figure 16: results for static strain analysis

The strain analysis results(fig. 16), visualized in blue throughout the structure, demonstrate that the scissor lift design operates well within allowable strain limits. This uniform blue coloration indicates that the strain distribution is even and remains below critical thresholds, confirming that the structural components will maintain their elastic behavior under normal operating conditions. The consistent strain pattern suggests effective load distribution across the mechanism's components, validating the design's ability to handle the specified operational loads without risk of permanent deformation. The Static Strain analysis of the lift was simulated with a two material for all the parts (Aluminum alloy 1066 and AISI Steel alloy) so that the region of max strain can be identified.

### **0.1.11 Agv chassis design and analysis report**

#### **0.1.11.1 Design Specifications**

The AGV chassis is designed to accommodate a maximum load capacity of 300 kg (2943N), with an additional safety margin factored into the structural calculations. The overall dimensions of 0.95m length, 0.68m width, and 0.4m height have been integrated into the design parameters to ensure optimal clearance and functionality while maintaining a low center of gravity for enhanced stability.

Key design specifications include:

- Maximum Load Capacity: 300 kg (2943N)
- Height: 0.4m
- Length: 0.95m
- Width: 0.68m
- Material: 40x40 aluminum alloy extrusion profiles
- Safety Factor: 1.5 for dynamic loading conditions

#### **0.1.11.2 Structural Configuration**

The AGV chassis employs a robust structural configuration designed for optimal stability and load distribution. The framework utilizes a combination of horizontal and vertical aluminum profiles, strategically arranged to create a rigid and durable support system. The design incorporates precise geometric relationships between components to ensure even weight distribution and minimize structural stress points. This configuration allows for efficient integration of all subsystems while maintaining the necessary strength-to-weight ratio

required for AGV operations. The modular nature of the structural layout also facilitates easy maintenance access and future modifications if needed.

The primary framework consists of:

- Horizontal Assembly: Four parallel 40x40 aluminum profiles arranged in rows
- Vertical Support: Eight column profiles providing structural integrity
- Connection Methods: Precision-engineered screw brackets (plate and corner types)
- Fastening System: High-grade bolts with specified torque requirements

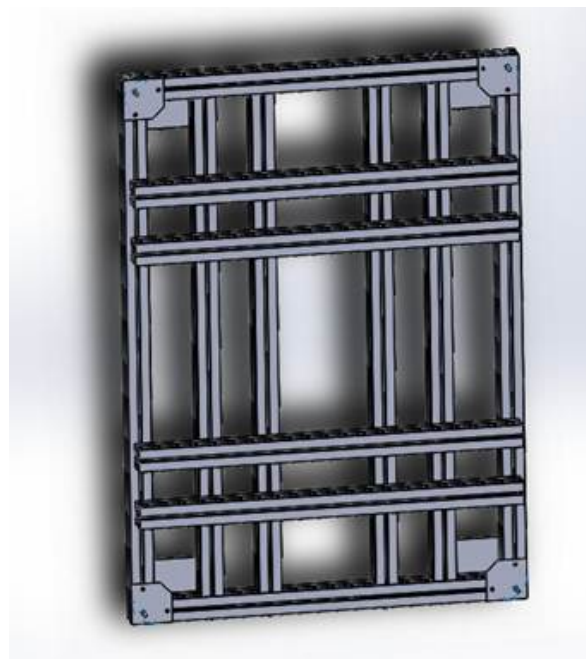


Figure 17: AGV chassis structure

#### 0.1.11.3 Component Integration

The chassis design incorporates multiple specialized zones for optimal integration of components and systems. The Central Integration Zone features a reinforced mounting platform specifically designed for the scissor lift mechanism, along with a centralized battery pit that ensures optimal weight distribution throughout the structure. For mobility systems, the chassis includes four castor wheel mounting points with reinforced brackets, two drive wheel installations complete with motor mount interfaces, and precision-aligned gear and bearing housing attachments. This layout maximizes structural integrity while maintaining efficient space utilization and accessibility for maintenance.

#### 0.1.11.4 Protective Framework

The NET-frame superstructure consists of a robust protective framework designed to safeguard internal components while maintaining accessibility. Four corner aluminum profile supports provide the primary structural integrity, while integrated transparent panels enable clear visibility of internal operations. Strategic access points are incorporated throughout the framework to facilitate routine maintenance and component replacement procedures.

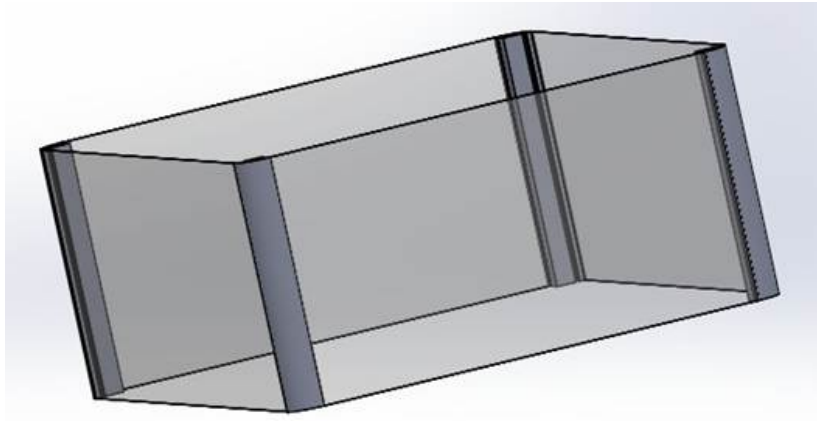


Figure 18: 3D model of protective frame and covering

#### 0.1.11.5 Design Methodology

The development process followed a systematic approach that began with comprehensive 2D design implementation using AutoCAD. This initial phase focused on precise dimensioning, critical clearance verification, and detailed component interface planning. The process then progressed to advanced 3D modeling using SolidWorks, enabling complete assembly visualization, thorough interference checking between components, and dynamic movement simulation to validate the design's functionality.

#### 0.1.11.6 Load Distribution Analysis

The static load distribution analysis revealed optimal weight distribution characteristics across all support points, with the chassis demonstrating minimal deflection under the maximum load capacity of 300 kg. Dynamic load considerations encompassed acceleration and deceleration forces, turning moment effects, and vibration damping characteristics, ensuring robust performance under various operational conditions.



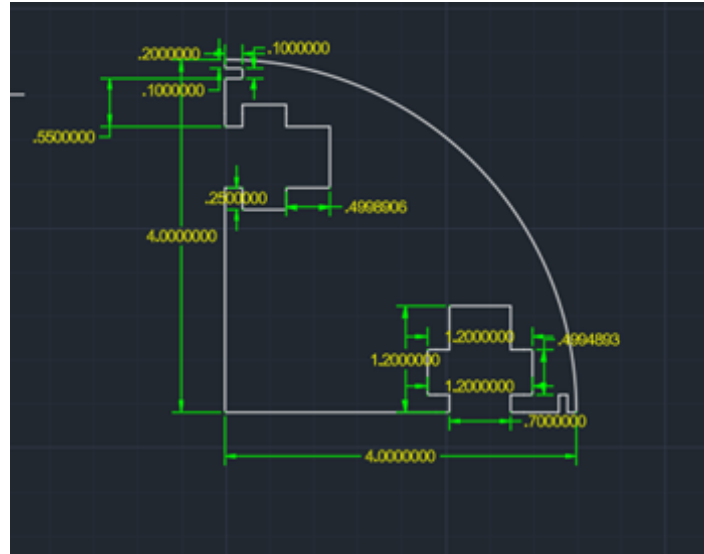


Figure 19: 2D profile of aluminum extrusion

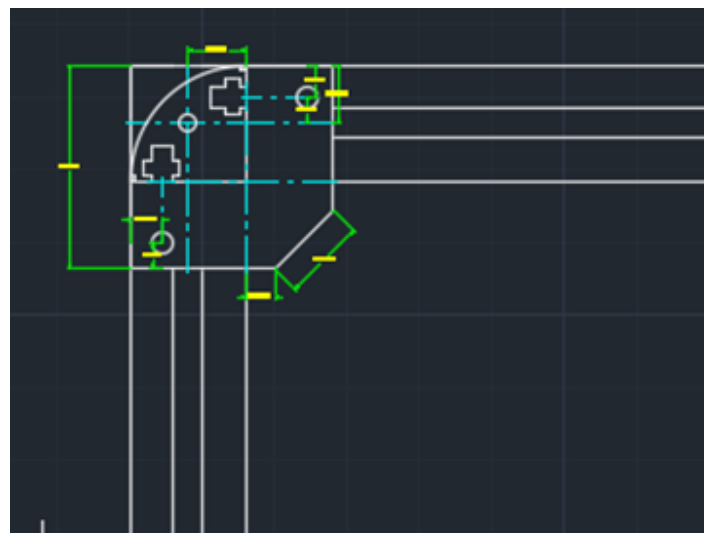


Figure 20: 2D model of profile joint and fasteners

#### 0.1.11.7 Symmetry Stress Analysis

Using SolidWorks Simulation, stress analysis validated the design's structural integrity, showing Von Mises stress values well within material limits. The results revealed uniform stress distribution with no significant concentration points. The structure exhibited acceptable maximum deflection ranges while maintaining elastic behavior under operational loads, with minimal torsional effects.

Comprehensive testing confirmed the chassis's structural stability under maximum load conditions, demonstrating seamless integration with scissor lift operations and effective weight distribution during movement. All integrated systems demonstrated proper functionality, validating the design's ability to meet operational requirements while maintaining necessary

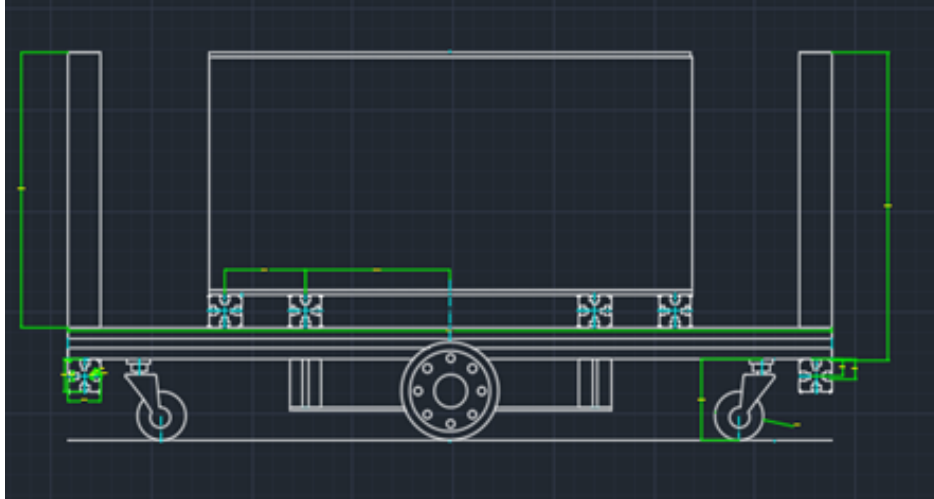


Figure 21: 2D model of Chassis and frame

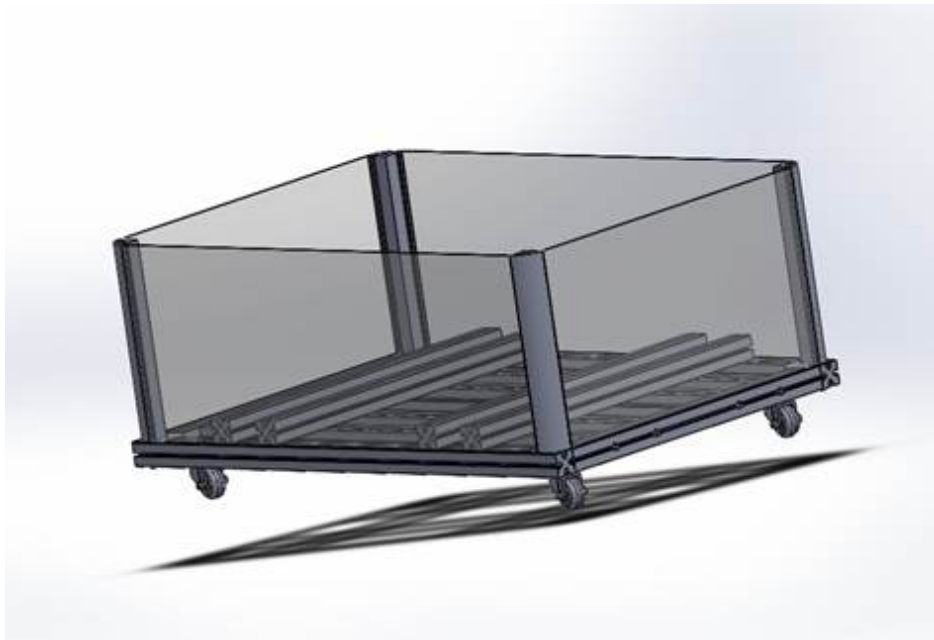


Figure 22: 3D design of chassis and frame covering

safety factors.

#### 0.1.11.8 Load Analysis with 2943N Force

The chassis undergoes extensive analysis under a total force of 2943N (equivalent to  $300\text{kg} \times 9.81 \text{ m/s}^2$ ). Each corner support bears approximately 735.75N, representing one-quarter of the total load. The central mounting points experience additional moment forces due to dynamic loading, while support beams are subject to combined axial and bending stresses.

The 40x40 aluminum extrusion profiles are engineered to handle substantial vertical load-

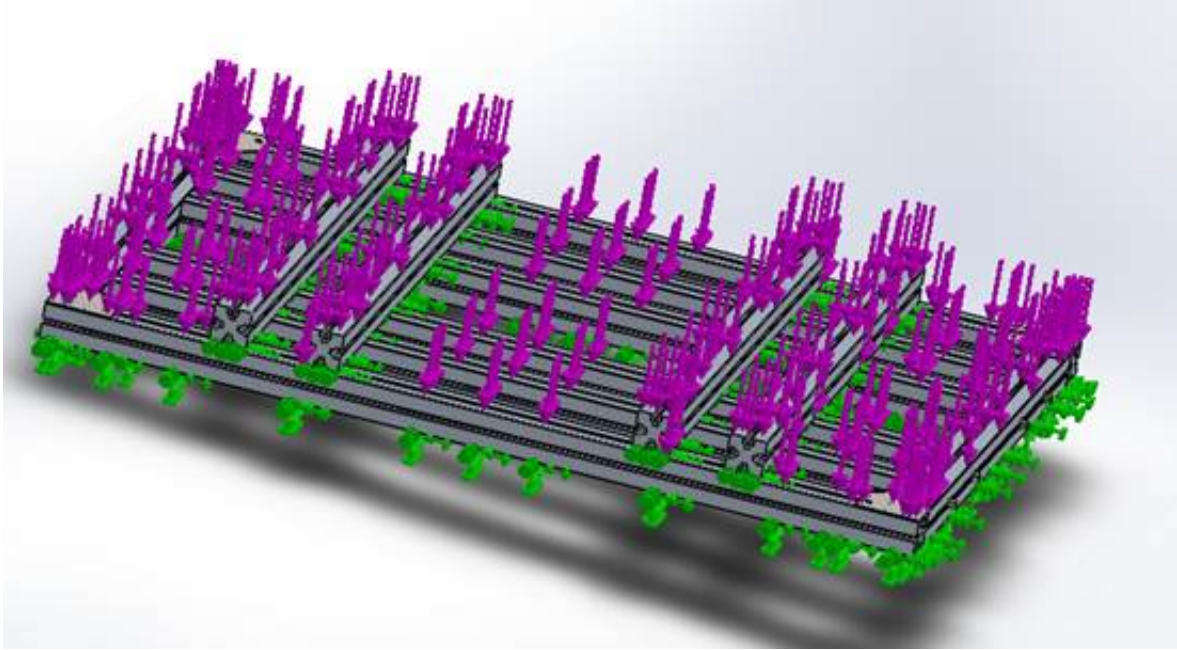


Figure 23: Load distribution on the chassis

ing, with direct compressive force of 2943N distributed across vertical supports. A safety factor of 1.5 is incorporated for dynamic loading conditions, with maximum allowable stress calculations adjusted accordingly. Horizontal forces, including shear forces during acceleration and deceleration, are carefully considered in the structural design.

Critical points analysis focuses on joint integrity, with particular attention to bracket connections experiencing increased stress concentrations. Bolt preload requirements are adjusted for higher forces, and weld points are designed to withstand greater cyclic loading. The increased load affects structural deformation, necessitating careful consideration of vertical deflection patterns and their impact on component alignment.

To ensure safety under the 2943N load, comprehensive structural reinforcement measures are implemented, including additional support brackets at high-stress points, increased material thickness in critical areas, and enhanced joint design for optimal load distribution. This thorough analysis ensures the chassis maintains structural integrity and operational safety under specified load conditions.